



HAL
open science

Cellulose Depolymerization with LPMO-inspired Cu Complexes

Ivan Castillo, Andrea Torres-Flores, Diego Abad-Aguilar, Armando Berlanga-Vázquez, Maylis Orio, Diego Martínez-Otero

► **To cite this version:**

Ivan Castillo, Andrea Torres-Flores, Diego Abad-Aguilar, Armando Berlanga-Vázquez, Maylis Orio, et al.. Cellulose Depolymerization with LPMO-inspired Cu Complexes. *ChemCatChem*, 2021, 13 (22), pp.4700-4704. 10.1002/cctc.202101169 . hal-03862129

HAL Id: hal-03862129

<https://hal.science/hal-03862129>

Submitted on 30 Nov 2022

HAL is a multi-disciplinary open access archive for the deposit and dissemination of scientific research documents, whether they are published or not. The documents may come from teaching and research institutions in France or abroad, or from public or private research centers.

L'archive ouverte pluridisciplinaire **HAL**, est destinée au dépôt et à la diffusion de documents scientifiques de niveau recherche, publiés ou non, émanant des établissements d'enseignement et de recherche français ou étrangers, des laboratoires publics ou privés.

Cellulose Depolymerization with LPMO-inspired Cu Complexes

Ivan Castillo,^{*[a]} Andrea P. Torres-Flores,^[a] Diego F. Abad-Aguilar,^[a] Armando Berlanga-Vázquez,^[a] Maylis Orio,^[b] and Diego Martínez-Otero^[c]

[a] Prof. Ivan Castillo, M. Sc. Andrea P. Torres-Flores, Diego F. Abad-Aguilar, M. Sc. Armando Berlanga-Vázquez
 Instituto de Química
 Universidad Nacional Autónoma de México
 Circuito Exterior, CU, 04510, México
 E-mail: joseivan@unam.mx
 https://i.quimica.unam.mx/dr-ivan-castillo-perez

[b] Prof. Maylis Orio
 Aix Marseille Université, CNRS, Centrale Marseille, iSm2,
 13397, Marseille, France

[c] Dr. Diego Martínez-Otero
 Centro Conjunto de Investigación en Química Sustentable UAEM-UNAM
 Carretera Toluca-Atlamulco km 14.5
 Toluca, 50200, Estado de México, México

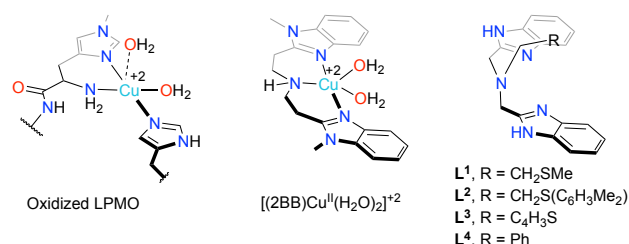
Supporting information for this article is given via a link at the end of the document.

Abstract: Bis(benzimidazole)amine-based copper complexes, with structural similarities to the active sites of Lytic Polysaccharide Monooxygenase enzymes (LPMOs), were tested for the oxidative degradation of cellulose. Spectroscopic characterization of the complexes, as well as structural authentication of one of them, confirm a tetragonal coordination environment with 3 nitrogen donors, as well as a thioether in axial positions. Aqueous oxidative degradation of cellulose was achieved with the Cu^{II} complexes and H₂O₂ as oxidant through putative cupric-hydroperoxo intermediates. Conversion of cellulose was achieved in up to 67% yield of soluble oligosaccharide derivatives at ambient temperature and pressure. The products were analyzed in aqueous solution by HPLC-MS, confirming oxidative depolymerization of cellulose under ambient conditions, in an analogous fashion to LPMOs.

Copper monooxygenase enzymes have been the object of increasing attention due to their ability to selectively hydroxylate C-H bonds, including those of recalcitrant substrates such as methane.^[1] Recently, the breadth of copper enzymes has extended to the family of Lytic Polysaccharide Monooxygenases (LPMOs),^[2] which cleave the glycosidic bonds of recalcitrant saccharides such as cellulose and chitin by an oxidative mechanism that results in polymer degradation.^[3,4] LPMOs are characterized by a monocopper site with three nitrogen donors, with a 'histidine brace' motif defined by an imidazole N-donor and a terminal amine, complemented by an additional histidine-derived imidazole, as shown in Scheme 1. The development of catalytic systems akin to LPMO would have technological impact for the use of recalcitrant biomass as a source of renewable feedstocks, including D-glucose and its derivatives.^[5] In addition, fundamental questions regarding the oxidizing co-substrate (dioxygen^[2] or hydrogen peroxide^[6]), the active copper-oxygen species,^[7] and the detailed mechanism of C-H activation remain to be answered.

A handful of inorganic model systems have been developed in attempts to gain insight on the mechanistic details of C-H activation that leads to polysaccharide degradation. Whether hydrogen peroxide acts as a shunt or as the true oxidant in biological systems, its use in conjunction with model copper complexes results in higher degradation activity in all cases. Two

model systems containing a mixed imidazole/pyridylamine-based donor set,^[8] and the bis(benzimidazole)amine-based **2BB**^[9] (Scheme 1), provide examples of confirmed oxidative degradation of model substrates. The more recently reported systems based on 2-pyridyl/diazepane,^[10] bis(imidazole)amine,^[11] and bis(2-picolyl)amine^[12] ligands degrade *p*-nitrophenolate-derivatized glucose and/or disaccharides, with the *p*-nitrophenolate leaving group quantified as the end product by UV-vis spectroscopy. In the first two cases, D-allose was also identified as product, instead of the expected gluconic acid upon hydrolysis of the initially formed gluconolactone; in the latter, the saccharide byproducts were not identified. Attempts to rationalize the catalytic activity of model complexes through analysis of physicochemical properties include correlations of the redox potential of the Cu^{III} couple. Nonetheless, even the systems with relatively low half-wave potentials ($E_{1/2}$) relative to those of LPMOs are active.^[8] In this regard, only the (**2BB**)Cu^{III} and bis(imidazole)amine-Cu^{III} systems have redox potentials that are within the range of LPMOs [155-370 mV relative to the Standard Hydrogen Electrode (SHE)],^[13] although (**2BB**)Cu^{III} was incorrectly identified as having a low $E_{1/2} = 76$ mV vs SHE.^[11]



Scheme 1. Active site of fungal LPMO, the model system [(**2BB**)Cu^{II}(H₂O)₂]⁺², and the benzimidazole-based ligands **L**¹-**L**⁴ employed in this work.

In light of the discrepancies mentioned above, and to provide more information of the types of systems that may oxidatively degrade the natural polysaccharide substrates to value-added chemicals such as oligo-, monosaccharides (D-glucose) and its dehydrated derivatives (5-hydroxymethylfurfural), we extended this chemistry to the previously reported bis(benzimidazole)amine-based ligands **L**²-**L**⁴ (in Scheme 1).^[14]

COMMUNICATION

The novel derivative **1** was prepared following the procedure reported previously for **L**²-**L**⁴, by introduction of the benzimidazole moieties to the nitrogen atom of 2-aminoethylmethylthioether with 2 equivs. of *N*-*tert*-butoxycarbonyl (BOC)-protected 2-chloromethylbenzimidazole. Deprotection of the *N*-BOC group with concentrated HCl, followed by neutralization, afforded **1** in 76% yield, see Figs. S1-S3 in the Electronic Supporting Information (ESI). The corresponding cupric complexes were synthesized under conditions reported for similar systems, with Cu(ClO₄)₂·6H₂O or Cu(SO₃CF₃)₂ as Cu^{II} sources.^[14] [**1**Cu(NCCH₃)(ClO₄)]ClO₄ (**1**) was thus obtained in 92% yield, X-ray quality crystals were obtained by slow evaporation of an acetonitrile solution. The complex crystallizes in the orthorhombic space group *Pbca*, revealing a pseudo-octahedral environment around the Cu^{II} center. The Cu1-N average distance of 1.958 Å to the benzimidazole donors, Cu1-N1 distance of 2.128(5) Å to the central amine, and Cu1-N6 of 2.021(6) Å to the acetonitrile molecule are not exceptional, as is the Cu1-S1 distance of 2.646(2) Å for an axial thioether donor bound to a Jahn-Teller distorted Cu^{II} ion. Full characterization and crystallographic data are presented in Figs. S4-S5, Tables S1 and S2 (ESI).

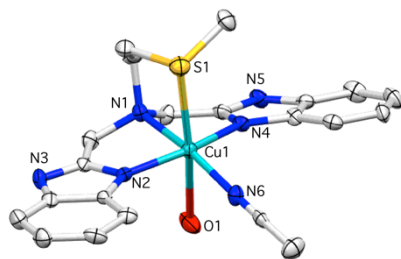


Figure 1. Mercury diagram of **1** at the 50% probability level, H atoms and perchlorate counterions (except for O1) omitted for clarity. Color code: C, grey; N, blue; O, red; Cl, green; S, yellow; Cu, turquoise.

Tetragonal geometry for **1** in solution was confirmed by Electron Paramagnetic Resonance (EPR) of the Cu^{II} center, acquired in acetonitrile at 77 K. The parameters determined, $g_{\perp} = 2.053$, $g_{\parallel} = 2.380$, $A_{\parallel} = 511$ MHz (Fig. S6), are similar to those reported for [**L**²Cu(ClO₄)₂] (**2**), [**L**³Cu(ClO₄)(H₂O)]ClO₄ (**3**), and [**L**⁴Cu(SO₃CF₃)₂] (**4**).^[14b] Electrochemical characterization of **1** by cyclic voltammetry (CV) was performed in acetonitrile, affording a half-wave potential of $E_{1/2} = 135$ mV relative to the ferrocenium/ferrocene (Fc⁺/Fc) couple, corresponding to the highest value among the complexes in this study (Fig. 2). On the other hand, **2** has the lowest value at $E_{1/2} = -115$ mV (Table 1), thus favoring the oxidized Cu^{II} form.

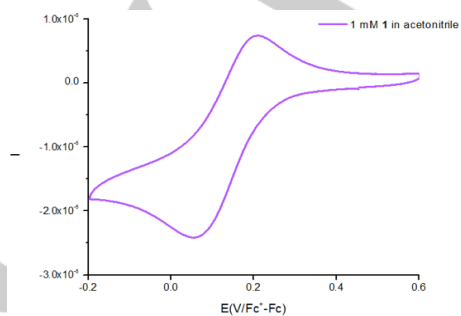


Figure 2. Cyclic voltammogram of 1 mM **1** in CH₃CN with 0.1 M [*n*-Bu₄N]PF₆ as electrolyte; glassy carbon electrode, scan speed 0.1 V s⁻¹.

Initial reactivity tests involved *in situ* reduction of **1**, **3**, and **4** with 1.5 equivs. of sodium ascorbate at room temperature in CH₃CN, evidenced by the disappearance of *d-d* transitions from 550 to 800 nm in UV-vis absorption spectra. Cooling to -30°C in a cryostat was followed by O₂ bubbling through the Cu^I solutions for one min; studies with **2** were precluded by its low solubility. For the rest of the complexes, no reactive copper-oxygen species could be discerned in the UV-vis spectra (Figs. S7-S9, ESI), even if **3** and **4** should react with dioxygen based on their redox potentials.

Table 1. Anodic (E_a), cathodic (E_c), ΔE ($E_a - E_c$), and half-wave ($E_{1/2}$) potentials for Cu^I salt and **1-4** (mV vs Fc⁺/Fc).

Compound	E_a	E_c	ΔE	$E_{1/2}$
[Cu(NCCH ₃) ₄]ClO ₄	760	550	210	655
1	210	60	150	135
2 ^[a]	-60	-170	110	-115
3 ^[a]	-10	-160	150	-85
4 ^[a]	40	-190	230	-75

[a] From reference 13b.

Alternatively, we tested the reactions of **1-4** with H₂O₂ as oxidant. Hydrogen peroxide is suspected to be the true oxidant in LPMO catalysis, and in model systems it has commonly been employed in conjunction with triethylamine (NEt₃) as base to promote the formation of cupric-hydroperoxo (Cu^{II}-OOH) species.^[15] The use of methanol as solvent allowed monitoring the reaction at -80°C, since the reactions at -30°C did not reveal significant changes in the absorption spectra. Thus, 1:1 H₂O₂/NEt₃ methanolic solutions were added to the complexes at low temperature for analysis by UV-vis spectroscopy. Changes in the spectra were more evident than in the corresponding oxidations with O₂, particularly after the addition of 3 or more equivs. of H₂O₂/NEt₃, Figs. S10-S12. The most informative spectra correspond to those of **4** in the presence of 10 equivs. of oxidant, featuring absorption bands at 347 nm ($\epsilon = 1280$ M⁻¹ cm⁻¹) and 611 nm ($\epsilon = 570$ M⁻¹ cm⁻¹) that can be assigned to a putative Cu^{II}-OOH,^[16] Figs. 3 and 4. Based on its intensity, DFT calculations (see below) and previous reports, the band at 347 nm was assigned as a hydroperoxo to Cu^{II} Ligand to Metal Charge Transfer (LMCT) transition, while the band at 611 nm was assigned as a combination of charge transfer and *d-d* transitions.

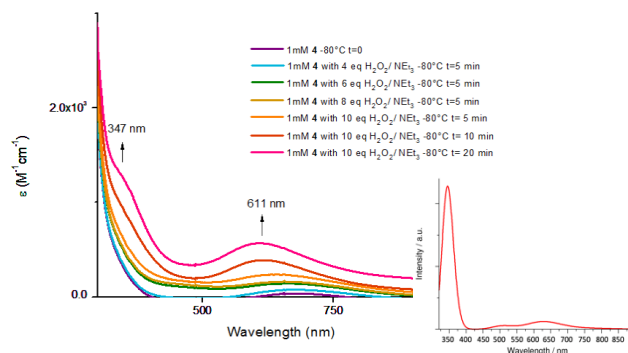


Figure 3. UV-vis spectra of 1 mM **4** in MeOH at -80°C upon addition of 1:1 H₂O₂/NEt₃ mixture (4-10 equivs.); inset: TD-DFT calculated UV-vis spectrum.

COMMUNICATION

Further support for the formation of cupric hydroperoxo $[L^nCu^{II}-OOH]^+$ species in the reactions between **1-4** and H_2O_2/NEt_3 was provided by EPR spectroscopy. This technique can discern the presence of monometallic Cu^{II} species in solution, relative to the bimetallic peroxo-bridged dicopper complexes that may also form under the experimental conditions described above.^[17] The latter species are expected to be EPR-silent, since the bridging peroxo ligands give rise to antiferromagnetically coupled cupric centers. Instead, addition of 10 equivs. of H_2O_2/NEt_3 to acetonitrile solutions of **1-4** resulted in EPR active species: the originally axial spectra give rise to isotropic ones at 77 K after addition of the oxidant, with $g_{iso} = 2.102$ to 2.107 (Figs. 4 and S13-S15). While no geometric information can be derived from the spectra, they are consistent with monometallic Cu^{II} species. Investigation of the properties of $[L^4Cu^{II}-OOH(CIO_4)]$ by DFT calculations involved geometry optimization of the parent **4**, validated by calculation of its redox potential at -70 mV (exp: -75 mV, Figs. S16-S21, Tables S3-S7). Geometry-optimized $[L^4Cu^{II}-OOH(CIO_4)]$ (Figs. 4, S22-S23) afforded an EPR calculated spectrum with $g_{iso} = 2.098$ (exp: 2.432102, Table S9) and main UV-vis features at 344 and 629 nm (exp: 347 and 611 nm, Figs. 3 and S24-S26 and Table S10), with the former assigned as $HOO \rightarrow Cu^{II}$ LMCT band.

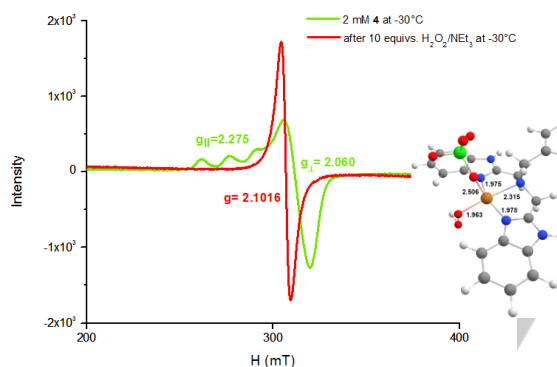


Figure 4. EPR spectrum of 2 mM **4** after addition of 10 equivs. H_2O_2/NEt_3 mixture at $-30^\circ C$ in acetonitrile (acquired at 77 K), and DFT-minimized structure of $[L^4Cu^{II}-OOH(CIO_4)]$ formed in the presence of H_2O_2/NEt_3 .

Once the potential reactive intermediate was identified as the putative cupric hydroperoxo complex, a protocol based on such conditions was adapted for testing the degradation of commercial cellulose. Thus, the use of **1-4** as catalyst precursors allowed us to undertake preparative scale degradation of 30 mg of cellulose in 2 mL of deionized water under benchtop conditions. $CuSO_4$, H_2O_2/NEt_3 mixture, and $CuSO_4/H_2O_2/NEt_3$ were tested as controls. Stirring for 24 h was followed by filtration to recover the unreacted cellulose to determine the conversion into soluble oligosaccharide derivatives (Fig. S27). In none of the control reactions was cellulose consumed, based on the weight of insoluble material recovered. In contrast, cellulose degradation was observed when 5% mol of complexes **1-4** were used, even in the absence of oxidant mixture, albeit in low yields, entries 1-4 in Table 2. Only marginal differences were observed after 24 and 72 h.

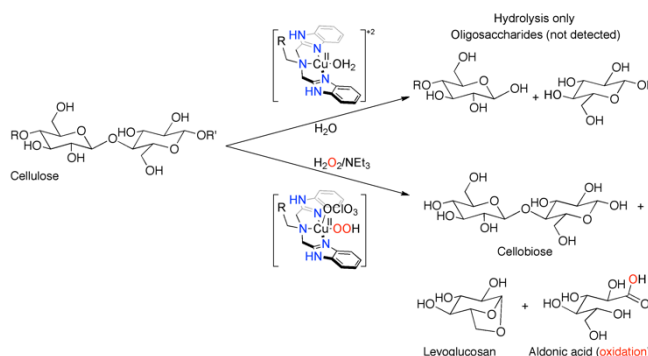
Two possibilities may account for the reactivity in the absence of H_2O_2/NEt_3 : the first one corresponds to hydrolysis by the Lewis acidic Cu^{II} centers.^[18] The second one would entail conversion of the Cu^{II} complexes to their cuprous analogs mediated by the reducing ends of cellulose.^[19] Cu^I complexes thus formed could

react with O_2 from air to oxidatively cleave the polysaccharide chain. The second option was discarded based on the reaction of complexes **1-4** with cellulose under inert atmosphere, resulting in similar degradation degree (4-15%); a hydrolytic mechanism may thus account for some percentage of the observed degradation in all cases. Complex **3** is most active for cellulose degradation in the absence of oxidant, with its ligand featuring a thiophene moiety that may be considered as poorly coordinating.^[14b] This may result in a Cu^{II} center with a hemilabile thiophene arm in **3**, and a more active catalyst for cellulose hydrolysis (14% after 72 h, entry 3 in Table 2). Catalyst performance improved upon addition of H_2O_2/NEt_3 , confirming the predominantly oxidative nature of the cellulose degradation, entries 5-8 in Table 2 and Scheme 2. An advantage of this method is that no pretreatment of cellulose is necessary,^[20] and that the reactions proceed at ambient temperature in open vessels. This contrasts with reports that require pretreatment, long reaction times, high temperature, pressure, and high catalyst loadings.^[21]

Table 2. Cellulose degradation (%) based on solid recovered.

Entry	Catalyst/Additives	% Consumed after 24 h	% Consumed after 72 h ^[c]
1	1 ^[a]	2	14
2	2	7	8
3	3	10	14
4	4	3	6
5	1 / H_2O_2/NEt_3 ^[b]	8	27
6	2 / H_2O_2/NEt_3	12	14
7	3 / H_2O_2/NEt_3	31	67
8	4 / H_2O_2/NEt_3	18	36

[a] 5% mol of catalyst used. [b] 5% mol of catalyst and 0.5 equiv. of H_2O_2/NEt_3 relative to cellulose. [c] A second load of 0.5 equiv. of H_2O_2/NEt_3 was added after 24 h for entries 5-8.



Scheme 2. Oxidative depolymerization of cellulose catalyzed by **1-4**; R and R' represent the polymer chains of cellulose.

Characterization of soluble products was undertaken by HPLC-MS. Filtration of the aqueous phase through a short plug of Celite to eliminate the catalysts resulted nonetheless in intense peaks corresponding to ligands and their fragments in some chromatograms, that are attributed to catalyst decomposition.

Despite these peaks, analysis of soluble degradation samples of $1/\text{H}_2\text{O}_2/\text{NEt}_3$ revealed chromatograms with byproducts such as ONeEt_3 as a result of the oxidation of NEt_3 (detected as $[\text{HONeEt}_3]^+$, Figs. S27, S28), along with the disodium adducts of aldonic acid and cellobiose at long retention times ($rt = 23.88$, Fig. S28, Scheme 2). The low activity of **2** under the conditions employed is likely due to its low aqueous solubility (Table 2), which did not make it amenable to HPLC-MS analysis.

In the case of the most active catalyst **3**, HPLC analysis shows virtually no soluble compounds present in the aqueous phase without oxidant mixture $\text{H}_2\text{O}_2/\text{NEt}_3$, Fig. S29a; the only peak identifiable by ESI-MS at $rt = 14.58$ (Fig. S29b) was assigned as protonated L^3 at $m/z = 374.15$. Similar results were obtained in the absence of oxidant with **4**, revealing only protonated L^4 at $m/z = 368.2$. Soluble products obtained in the presence of $\text{H}_2\text{O}_2/\text{NEt}_3$ were analyzed in the same manner, and the results lend further support for the oxidative cleavage of cellulose, as opposed to a hydrolytic transformation. Samples of cellulose treated with $3/\text{H}_2\text{O}_2/\text{NEt}_3$ resulted in chromatograms that differ significantly from those obtained from **3** alone: $[\text{HONeEt}_3]^+$ ($rt = 1.86$), $[\text{L}^3\text{H}]^+$ ($rt = 14.53$) and degradation fragments at $rt = 11.76, 22.37$, were detected along with peaks assigned to protonated levoglucosan ($rt = 4.90$, $m/z = 163.05$), cellobiose ($rt = 19.05$, $m/z = 343.13$), and the disodium adduct of gluconic acid ($rt = 23.86$, $m/z = 242.29$, Fig. S30 and Scheme 2). Similar fragments and cellulose degradation products were detected when **4** was employed as catalyst (Fig. S31). Although these results that challenges remain, such as the higher sensitivity for species that are readily protonated like the amines employed as ligands, and that higher glucose oligomers that may be present in solution after hydrolysis or oxidative cleavage cannot be detected,^[22] the feasibility to employ relatively simple cupric complexes as catalysts for cellulose degradation under benchtop conditions is encouraging.

In summary, benzimidazole-based copper complexes with coordination environments and redox potentials similar to those in LPMO monooxygenase enzymes are competent cellulose degradation catalysts under mild conditions, with $\text{Cu}^{\text{II}}\text{-OOH}$ species forming in the presence of $\text{H}_2\text{O}_2/\text{NEt}_3$ as oxidant mixture. Combined quantification of the remaining insoluble substrate that is not consumed during the reaction and analysis of the soluble portion by HPLC-MS provides information of the oxidative degradation of cellulose. The possibility to extend this strategy to recalcitrant substrates such as chitin and lignocellulose with the complexes herein reported, as well as LPMO-inspired derivatives, is currently under investigation in our laboratory.

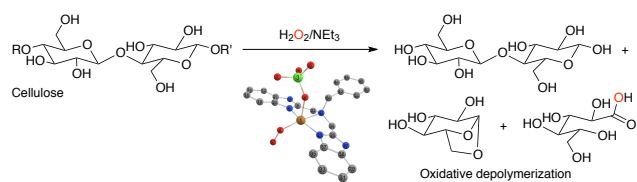
Acknowledgements

The authors thank Simón Hernández-Ortega for crystallographic assistance, Virginia Gómez-Vidales for EPR spectroscopy, Lucero Ríos and María del Carmen García for mass spectrometry, María de la Paz Orta for combustion analysis, Everardo Tapia for HPLC-MS, DGAPA-PAPIIT (IN217020), Conacyt-ECOS Nord (291247) and Conacyt (A1-S-8682, Beca 778895) for financial support.

Keywords: biomass • catalysis • LPMO • biomimetic • copper

- [1] a) C. Bédard, R. Knowles, *Microbiol. Rev.* **1989**, *53*, 68-84; b) R. L. Lieberman, A. C. Rosenzweig, *Nature* **2005**, *434*, 177-182.
- [2] G. Vaaje-Kolstad, B. Westereng, S. J. Horn, Z. Liu, H. Zhai, M. Sortie, V. G. H. Eijsink, *Science* **2010**, *330*, 219-222.
- [3] R. J. Quinlan, M. D. Sweeney, L. Lo Leggio, H. Otten, J.-C. N. Poulsen, K. S. Johansen, K. B. R. M. Krogh, C. I. Jorgensen, M. Tovborg, A. Anthonsen, T. Tryfona, C. P. Walter, P. Dupree, F. Xu, G. J. Davies, P. H. Walton, *Proc. Natl. Acad. Sci. USA* **2011**, *108*, 15079-15084.
- [4] C. M. Phillips, W. T. Beeson IV, J. H. Cate, M. A. Marletta, *ACS Chem. Biol.* **2011**, *6*, 1399-1406.
- [5] a) G. Muller, A. Várnai, K. Salomon Johansen, V. G. H. Eijsink, S. J. Horn, *Biotechnol. Biofuels* **2015**, *8*, 187-195; b) J. Y. Lee, K. D. Karlin, *Curr. Opin. Chem. Biol.* **2015**, *25*, 184-193; c) K. K. Meier, S. M. Jones, T. Kaper, H. Hansson, M. J. Koetsier, S. Karkehabadi, E. I. Solomon, M. Sandgren, B. Kelemen, *Chem. Rev.* **2018**, *118*, 2593-2635.
- [6] B. Bissaro, A. K. Rohr, G. Muller, P. Chylenski, M. Skaugen, Z. Forsberg, S. J. Horn, G. Vaaje-Kolstad, V. G. H. Eijsink, *Nat. Chem. Biol.* **2017**, *13*, 1123-1128.
- [7] C. E. Elwell, N. L. Gagnon, B. D. Neisen, D. Dhar, A. D. Spaeth, G. M. Yee, W. B. Tolman, *Chem. Rev.* **2017**, *117*, 2059-2107.
- [8] A. L. Concia, M. R. Beccia, M. Orio, F. T. Ferre, M. Scarpellini, F. Biaso, B. Gliugliarelli, M. Réglier, A. J. Simaan, *Inorg. Chem.* **2017**, *56*, 1023-1026.
- [9] A. C. Neira, P. R. Martínez-Alanis, G. Aullón, M. Flores-Alamo, P. Zerón, A. Company, J. Chen, J. B. Kasper, W. R. Browne, E. Nordlander, I. Castillo, *ACS Omega* **2019**, *4*, 10729-10740.
- [10] S. Muthuramalingam, D. Maheshwaran, M. Velusamy, R. Mayilmurugan, *J. Catal.* **2019**, *372*, 352-361.
- [11] A. Fukatsu, Y. Morimoto, H. Sugimoto, S. Itoh, *Chem. Commun.* **2020**, *56*, 352-361.
- [12] Z. Yu, Z. Thompson, S. L. Behnke, K. D. Fenk, D. Huang, H. S. Shafaat, J. A. Cowan, *Inorg. Chem.* **2020**, *59*, 11218-11222.
- [13] V. V. Vu, S. T. Ngo, *Coord. Chem. Rev.* **2018**, *368*, 134-157.
- [14] a) P. R. Martínez-Alanis, M. López Ortiz, I. Regla, I. Castillo, *Synlett* **2010**, 423-426; b) L. A. Rodríguez Solano, I. Aguiñiga, M. López Ortiz, R. Tiburcio, A. Luviano, I. Regla, E. Santiago-Osorio, V. M. Ugalde-Saldívar, R. A. Toscano, I. Castillo, *Eur. J. Inorg. Chem.* **2011**, 3454-3460.
- [15] H. Ohtsu, S. Itoh, S. Nagatomo, T. Kitagawa, S. Ogo, Y. Watanabe, S. Fukuzumi, *Inorg. Chem.* **2001**, *40*, 3200-3207.
- [16] a) P. Chen, K. Fujisawa, E. I. Solomon, *J. Am. Chem. Soc.* **2000**, *122*, 10177-10193; b) T. Fujii, A. Naito, S. Yamaguchi, A. Wada, Y. Funahashi, K. Jitsukawa, S. Nagatomo, T. Kitagawa, H. Masuda, *Chem. Commun.* **2003**, 2700-2701.
- [17] N. Kitajima, K. Fujisawa, Y. Moro-oka, *J. Am. Chem. Soc.* **1989**, *111*, 8976-8978.
- [18] a) S. Striegler, N. A. Dunaway, M. G. Gichinga, J. D. Barnett, A.-G. D. Nelson, *Inorg. Chem.* **2010**, *49*, 2639-2648; b) S. Striegler, J. D. Barnett, N. A. Dunaway, *ACS Catal.* **2012**, *2*, 50-55; c) S. R. Kamireddy, J. Li, M. Tucker, J. Degenstein, Y. Ji, *Ind. Eng. Chem. Res.* **2013**, *52*, 1775-1782.
- [19] S. Kongruang, M. J. Han, C. I. Gil Breton, M. H. Penner, *Appl. Biochem. Biotechnol.* **2004**, *113*, 213-231.
- [20] B. Yang, C. E. Wyman, *Biofuels, Bioprod. Biorefin.* **2008**, *2*, 26-40.
- [21] a) A. S. Amarasekara, B. Wiredu, *Catal. Sci. Technol.* **2016**, *6*, 426-429; b) Y.-B. Huang, T. Yang, Y.-J. Luo, A.-F. Liu, Y.-H. Zhou, H. Pan, F. Wang, *Catal. Sci. Technol.* **2018**, *8*, 6252-6262; c) I. Bodachivskyi, U. Kuzhiumparambil, D. B. G. Williams, *Catal. Sci. Technol.* **2019**, *9*, 4693-4701.
- [22] a) B. Westereng, J. W. Agger, S. J. Horn, G. Vaaje-Kolstad, F. L. Aachmann, Y. H. Stentrøm, V. G. H. Eijsink, *J. Chromatogr. A* **2013**, *1271*, 144-152; b) B. Westereng, M. Ø. Arntzen, F. L. Aachmann, A. Várnai, V. G. H. Eijsink, J. W. Agger, *J. Chromatogr. A* **2016**, *1445*, 46-54.

Entry for the Table of Contents



LPMO-inspired benzimidazole-based copper complexes oxidatively degrade cellulose to cellobiose, aldonic acid and levoglucosan as soluble products in the presence of hydrogen peroxide/triethylamine as oxidant mixture under mild conditions through initially formed cupric hydroperoxo intermediates.

Institute and/or researcher Twitter usernames: Ivan Castillo @IvanCas68864020, Maylis Orio @orio52503713